

Probing heavy element nucleosynthesis through electromagnetic observations

Gabriel Martínez-Pinedo
Nuclei in the Cosmos (NIC XVII),
Institute Basic Science, Daejeon, Korea
September 22, 2023



TECHNISCHE
UNIVERSITÄT
DARMSTADT



DFG**HFF**

Helmholtz Forschungsakademie Hessen für FAIR



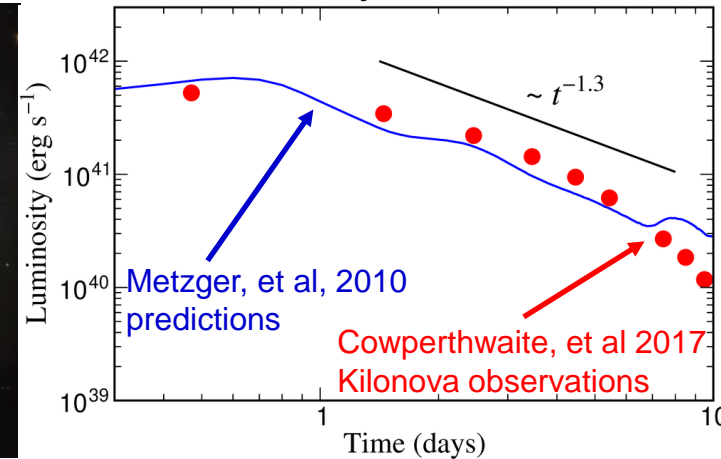
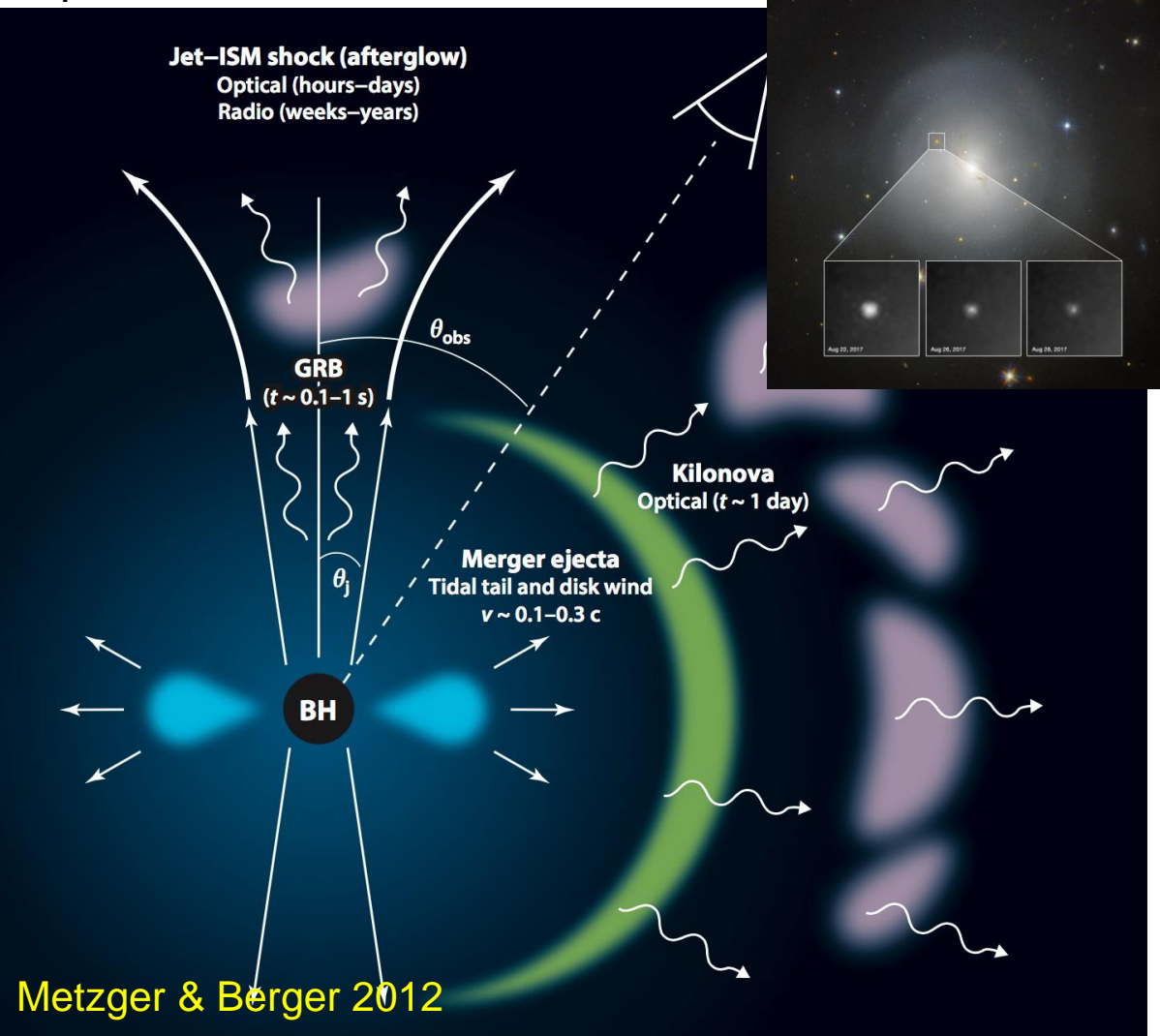
European Research Council
Established by the European Commission

ERC AdG KILONOVA



Kilonova: signature of the r-process

Kilonova: An electromagnetic transient due to long term radioactive decay of r-process nuclei

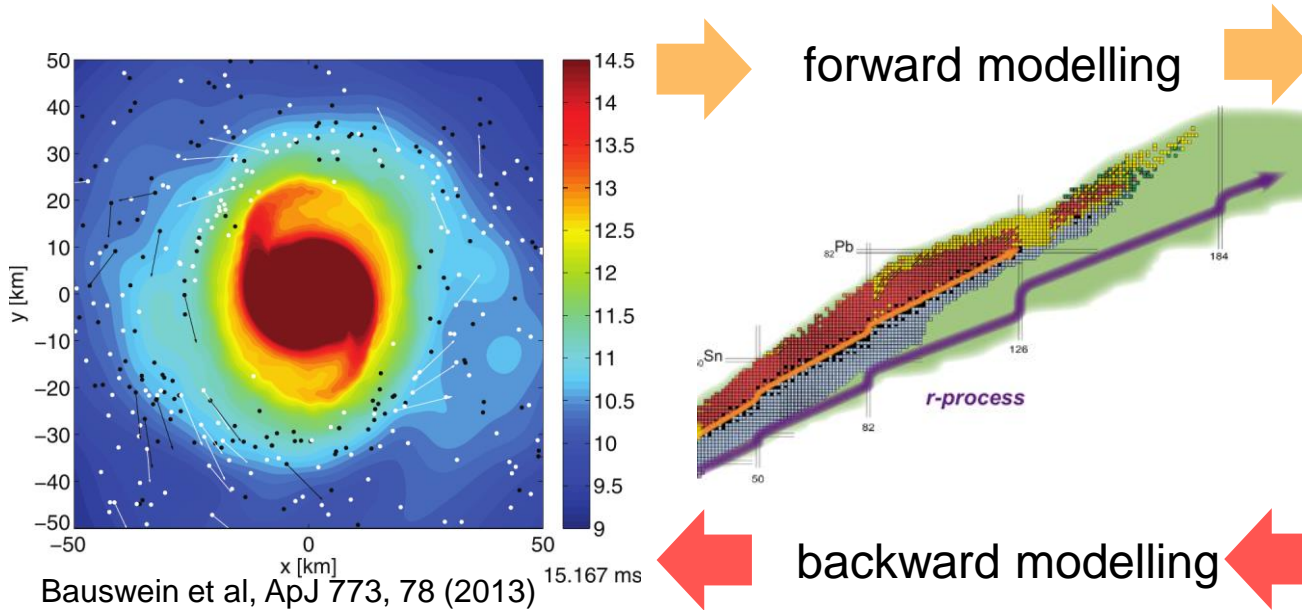


- Electromagnetic counterpart to Gravitational Waves
- Diagnostics physical processes at work during merger
- Direct probe of the formation r-process nuclei
- Information elements produced single event

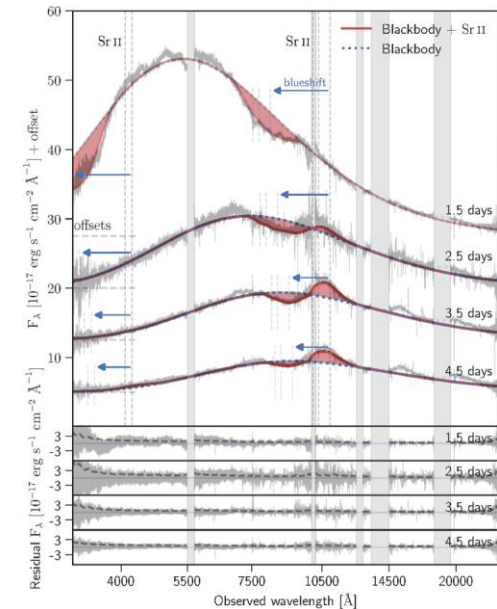
Pipeline for r-process in mergers

- Properties ejecta: proton-to-nucleon ratio (Y_e)
- Role of equation of state
- Role of neutrinos
- Physics of neutron-rich and heavy nuclei

- Radioactive energy deposition
- Thermalization decay products (Barnes+ 2016, Kasen+ 2019)
- Spectra formation: atomic data depends on ejecta evolution (LTE vs NLTE)

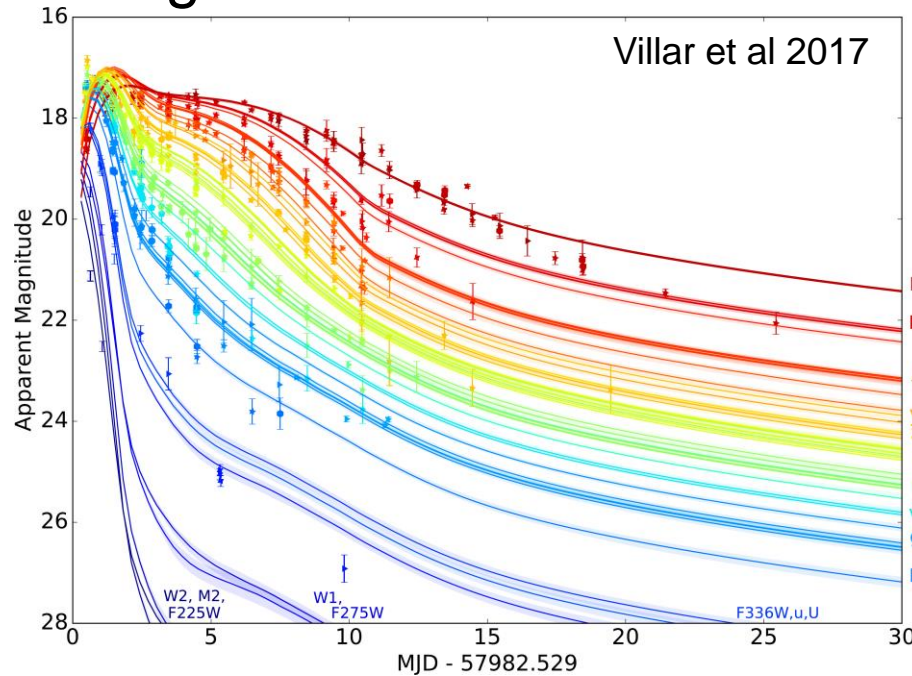


Infer components ejecta (Y_e)



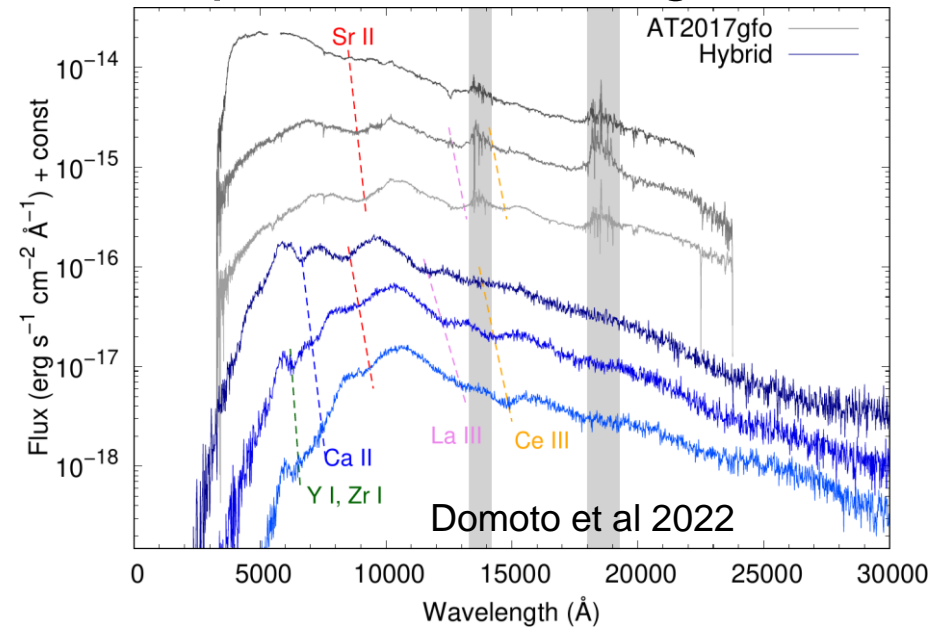
- Which r-process elements are produced in mergers?
- Are mergers the (main) r-process site?

Light curve



- **Complete** transition data: total opacity
- Color evolution: High vs Low opacity material
- Presence of Lanthanides/Actinides (high opacity)

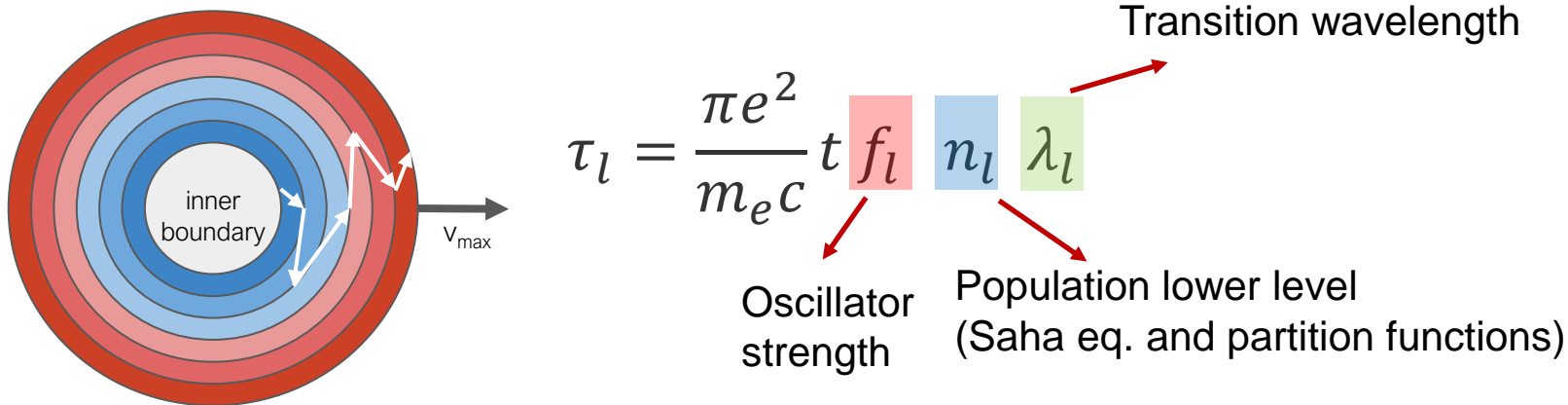
Spectral modelling



- Accurate data
 - LTE: line list bound-bound transitions
 - NLTE: + electron ion and photoionization cross sections, recombination coef
- Several elements observed
Sr (Watson+22), Y, Zr, La, Ce (Domoto+22, Gillanders+23, Snepken+23)

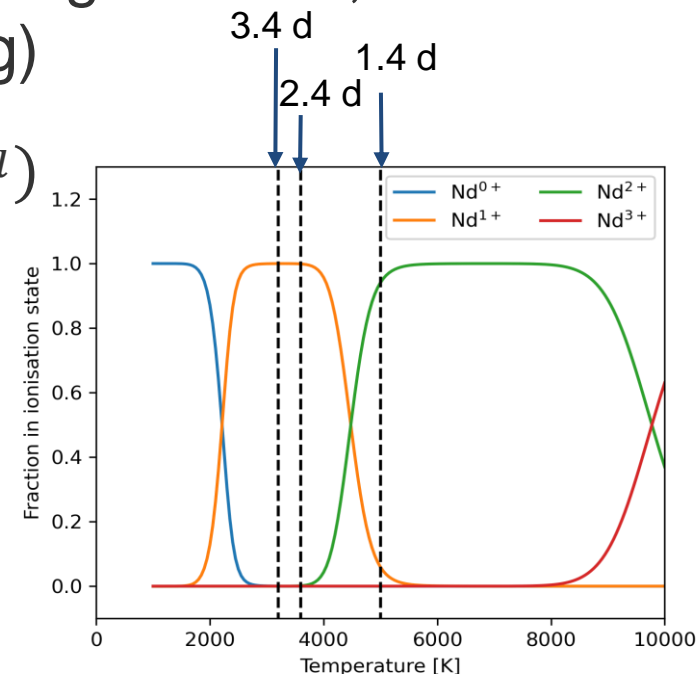
Atomic Opacities (LTE)

Sobolev optical depth (for a line l)



Expansion opacity (homologous expanding material, not used in the radiation transport modelling)

$$\kappa_{\text{exp}}^{\text{bb}} = \frac{1}{\rho c t} \sum_l \frac{\lambda_l}{\Delta \lambda_{\text{bin}}} (1 - e^{-\tau_l})$$



A. Flörs

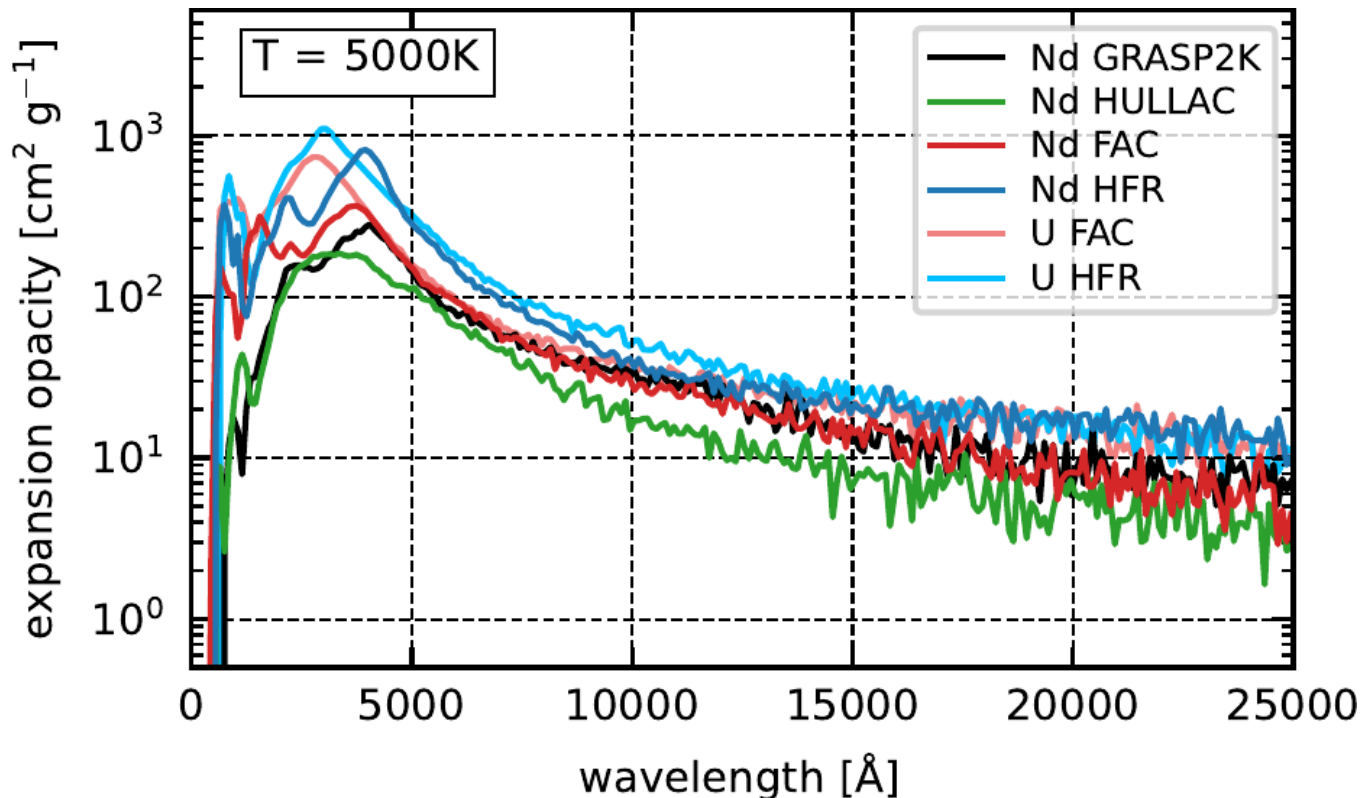
G. Leck

R. Silva



Goal: Develop database
well calibrated atomic
opacities

- U has larger opacity than Nd (similar behaviour expected for other Actinides)
- Confirmed by independent calculations HFR code (U. Mons) and Los Alamos suite (Fontes+2023)

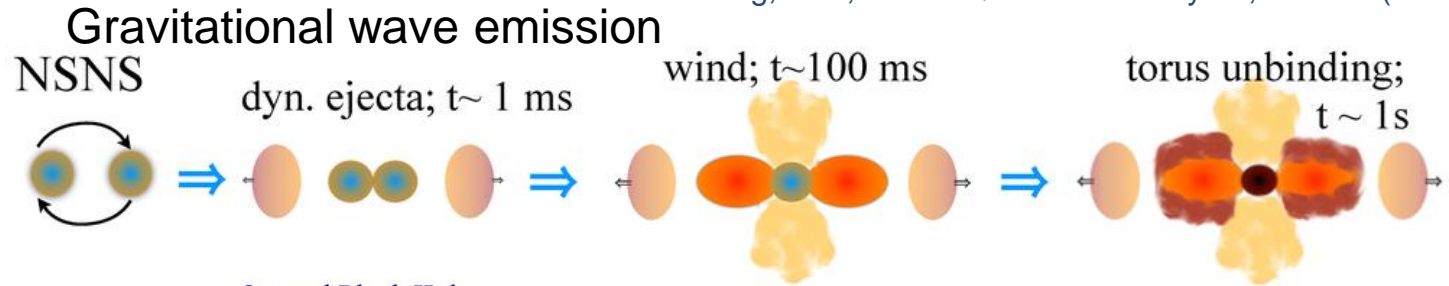


Silva et al, Atoms 10, 18 (2022); Flörs, Silva, et al, MNRAS 524, 3083 (2023)

Offers a method to identify presence of Actinides in spectra.

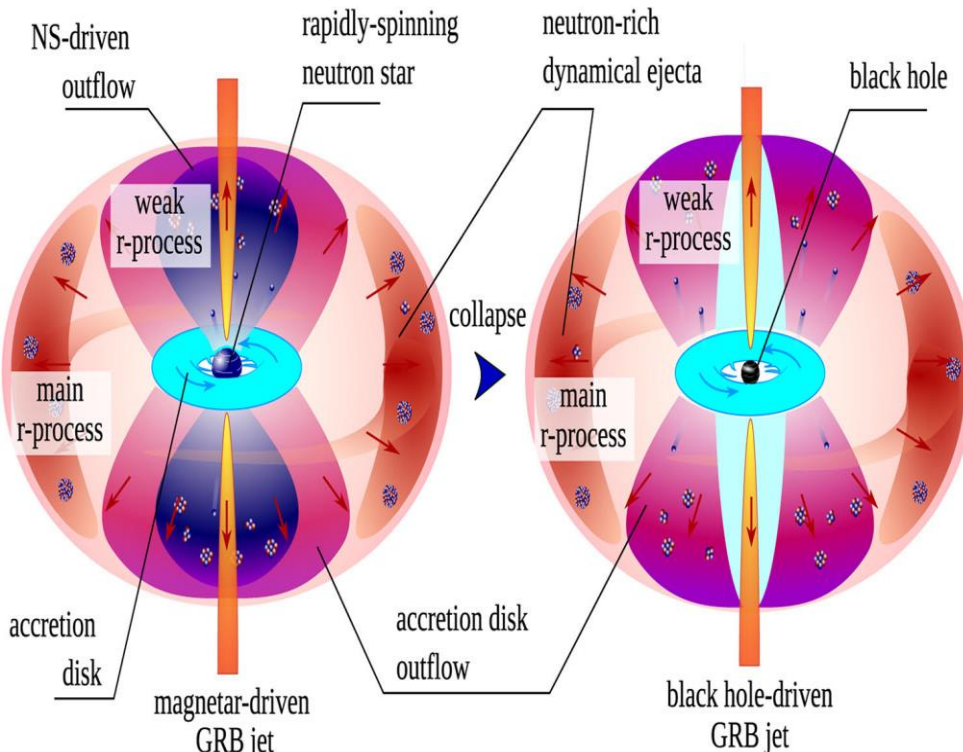
Neutron star mergers: Different ejection mechanisms

S. Rosswog, et al, Class. Quantum Gravity 34, 104001 (2017).

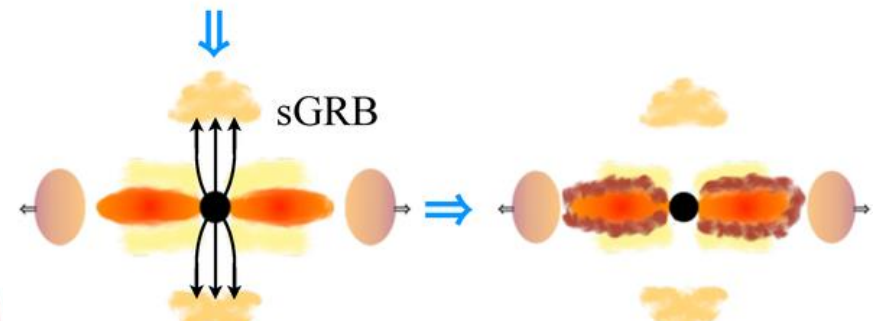


Central Neutron Star

Central Black Hole



BH formation



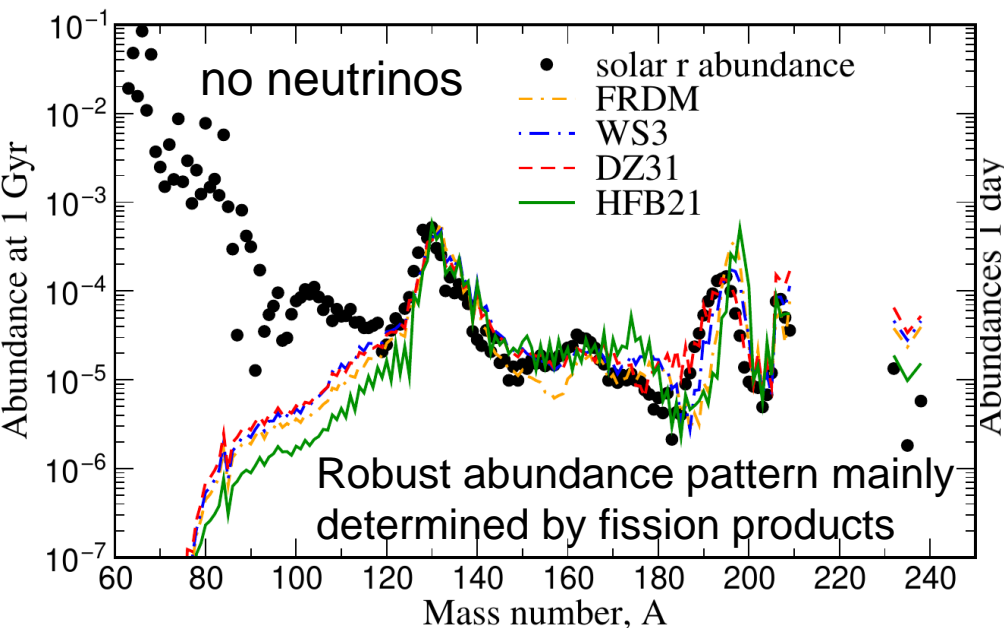
Two sources of ejecta:

- Dynamical during the early phases of the merger ($M \lesssim 0.01 M_{\odot}$)
- Accretion disc on longer timescales ($M \lesssim 0.05 M_{\odot}$)
- Lifetime neutron-star determines impact neutrinos

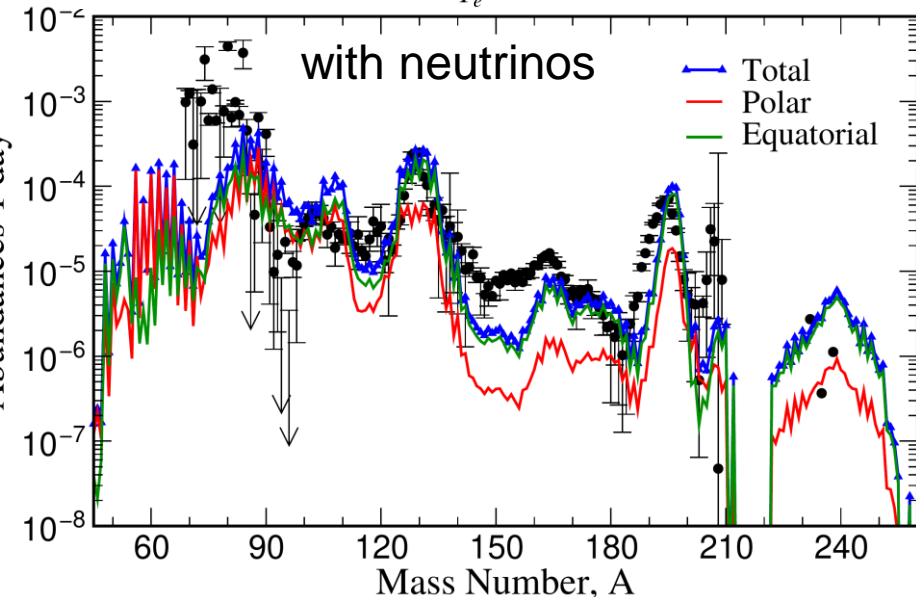
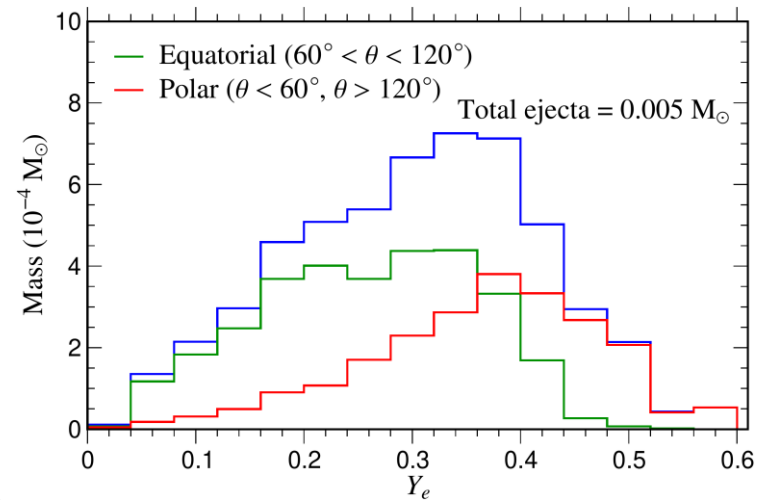
S. Rosswog and O. Korobkin, Annalen Der Physik **2022**, 2200306 (2022).

Dynamical ejecta (simulations)

- Initially dynamical ejecta was assumed to be very neutron rich ($Y_e \lesssim 0.1$).
- Starting with the work of Wanajo et al 2014, several studies have shown that weak processes modify the neutron-to-proton ratio
- Largest impact in the polar regions



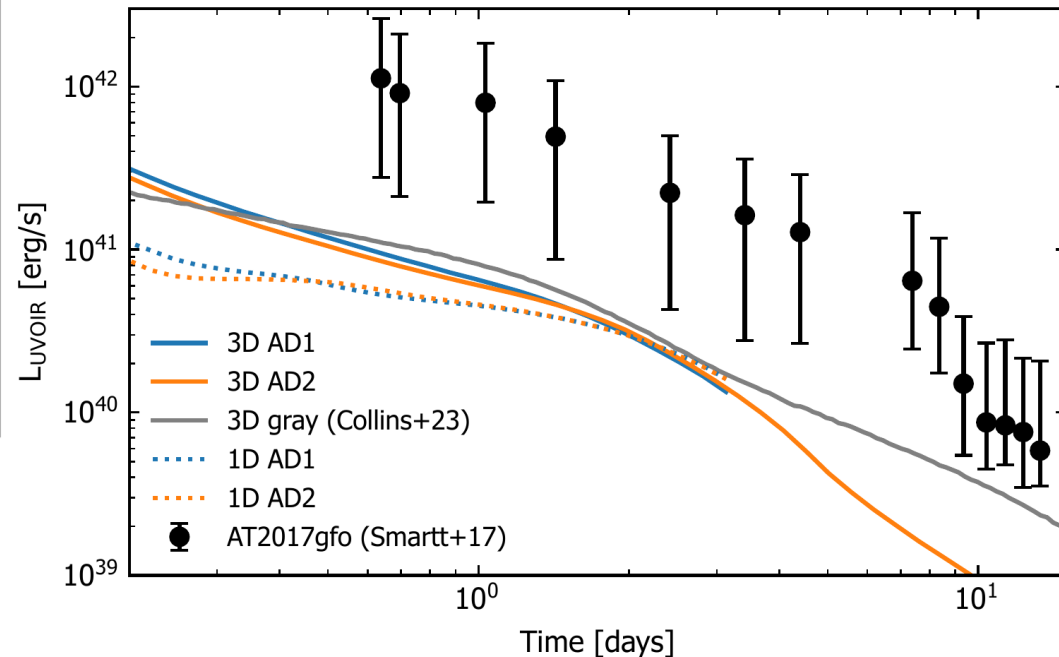
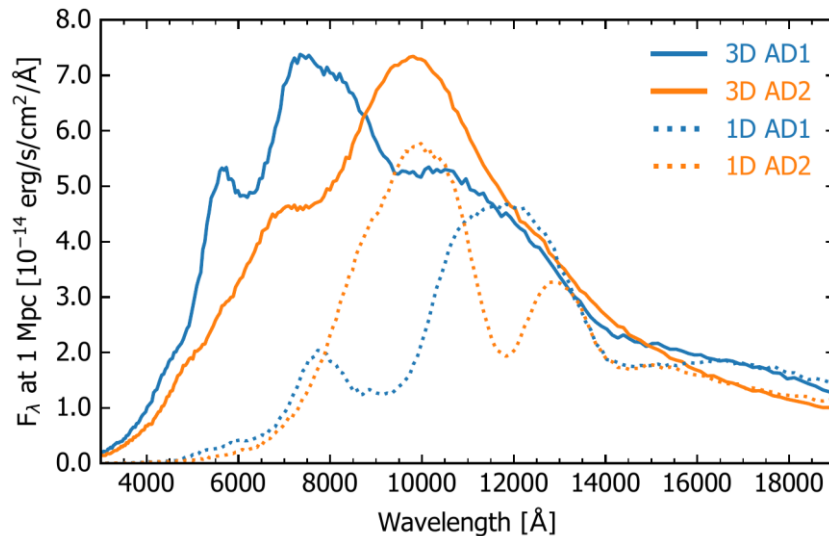
SPH Simulation **Vimal Vijayan**
 Neutrino transport: ILEAS
 1.35 – 1.35 M_{\odot} , SFHo EoS



Mendoza-Temis, et al, PRC 92, 055805 (2015)

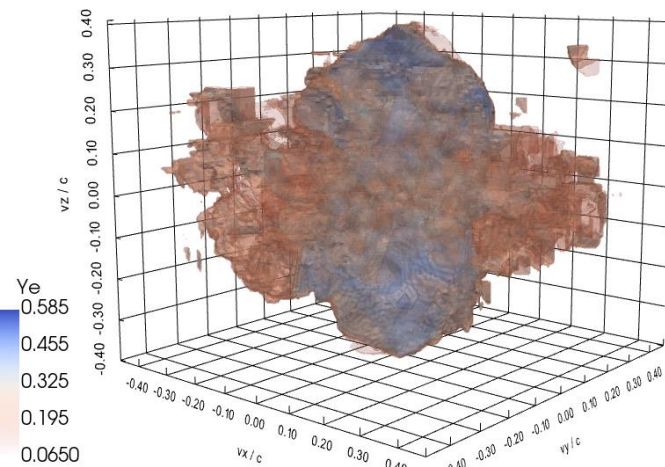
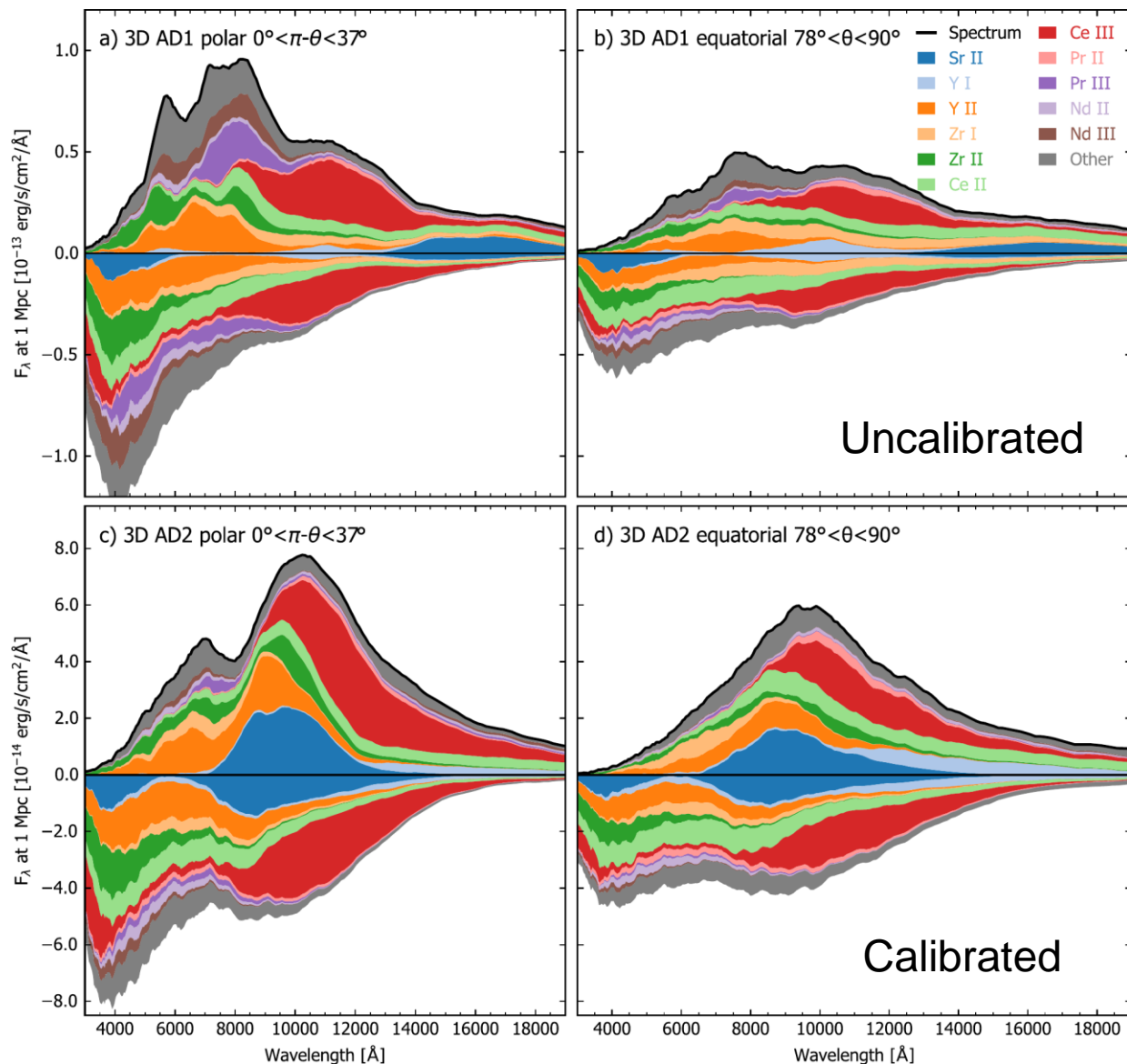


- Monte Carlo 3D radiative transfer using the ARTIS code.
<https://github.com/artis-mcrt/artis>
- Matter distribution based on SPH Dynamical ejecta ($0.005 M_{\odot}$)
- LTE simulation: follows 2591 nuclei (283 ions with gamma-ray transport and electron thermalization, 44 millions atomic transitions lines
AD1: Japan-Lithuania database Z=28-88, Tanaka+ 2020
AD2: AD1 + calibrated lines for Sr, Y, and Zr, Kurucz 2018



Shingles et al, ApJ 954, L41 (2023)

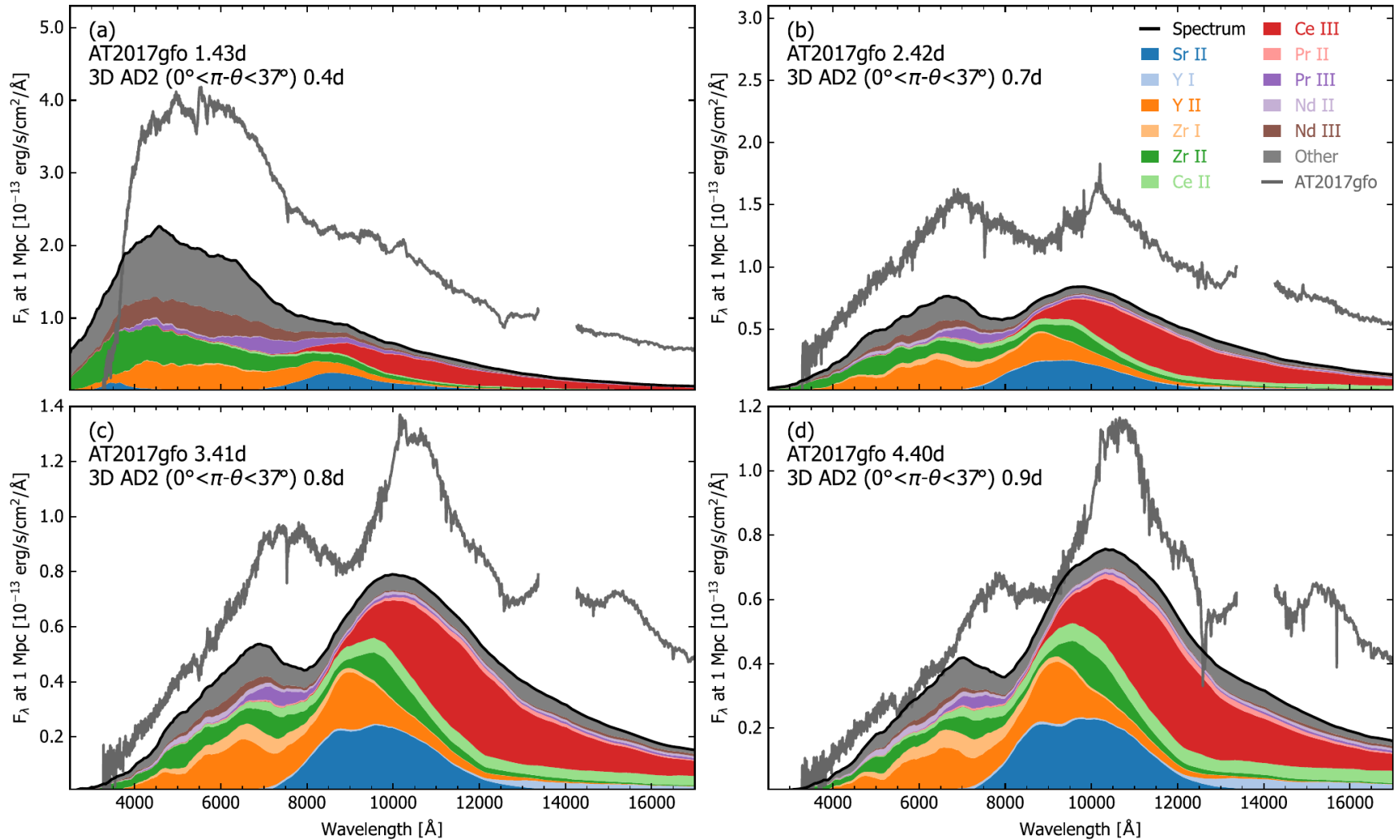
Angular dependence spectra



Differences reflect directional dependence of nucleosynthesis yields

Shingles et al, ApJ 954, L41 (2023)

Comparison AT2017gfo

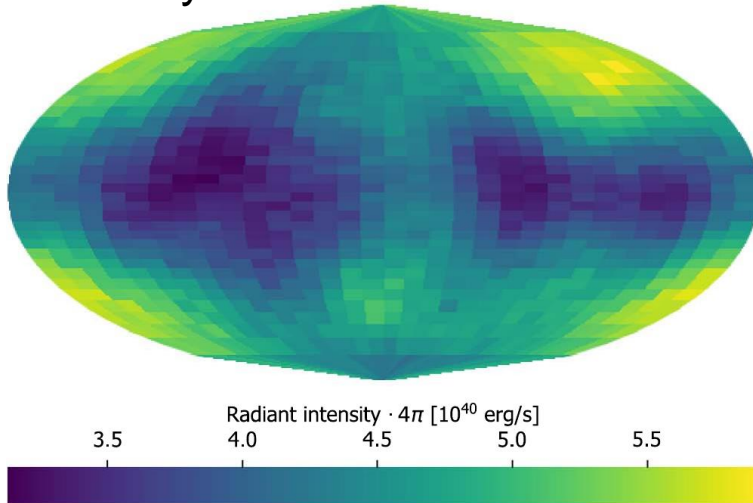


Similar spectral evolution that AT2017gfo once differences in brightness are accounted

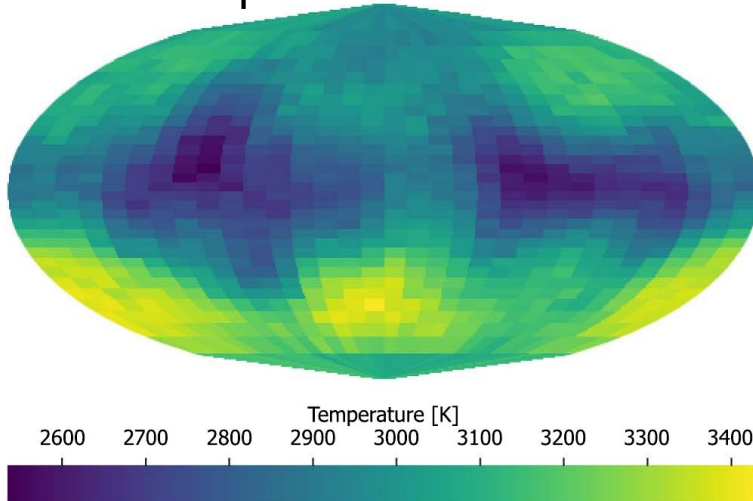
Shingles et al, ApJ 954, L41 (2023)

Asymmetry observables

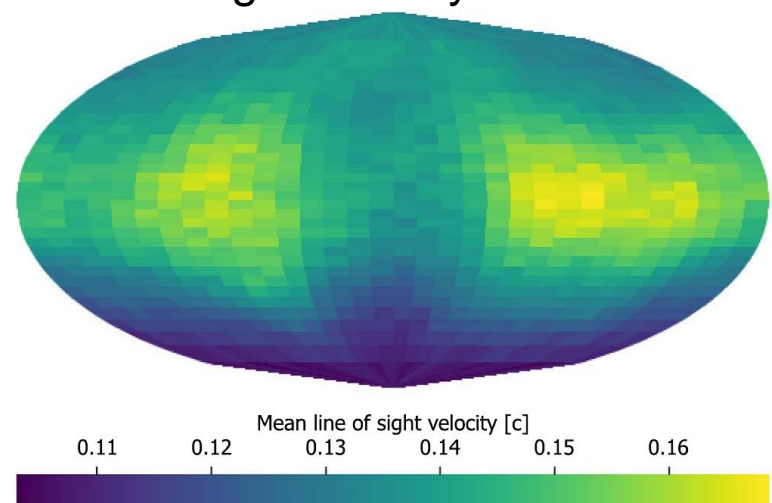
Intensity



Mean temperature



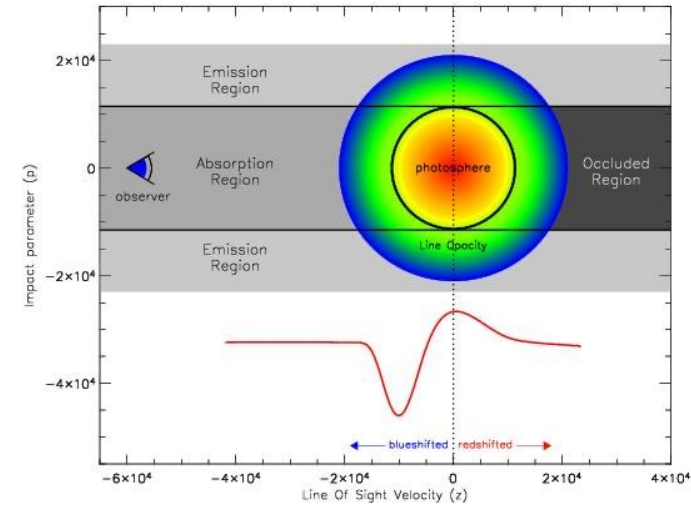
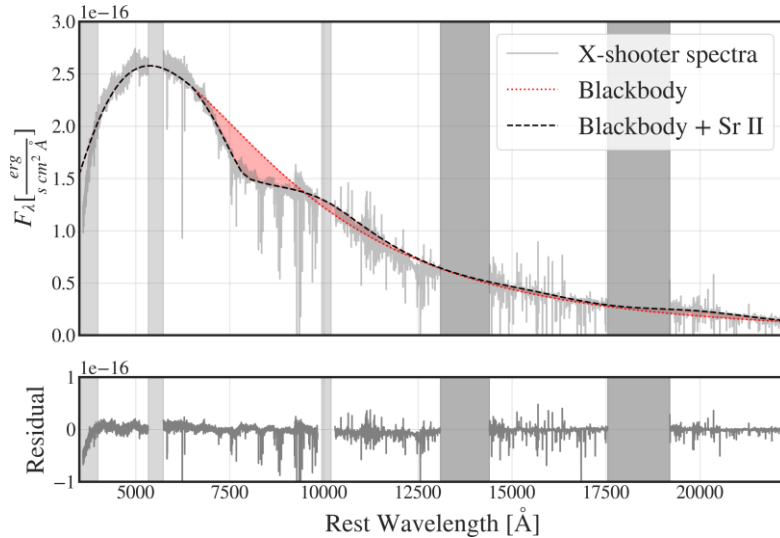
Line-of-sight velocity



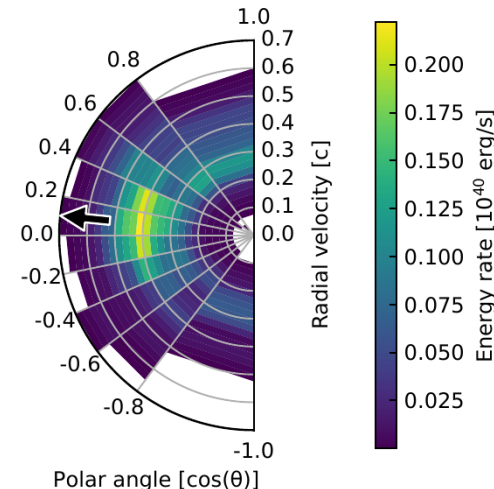
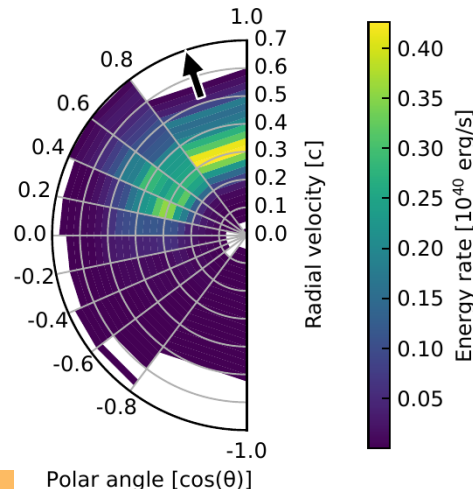
- Strong asymmetry observables
- Is this consistent with observations?

Shingles et al, ApJ 954, L41 (2023)

Analysis of AT2017gfo Sr II P-Cygni feature shows kilonova is highly spherical at early epochs [Sneppen et al, Nature 614, 436 (2023)]



Similar analysis based on 3D radiative transfer simulations suggest sphericity depends on observer line of sight [Collins et al, arXiv:2309.05579]

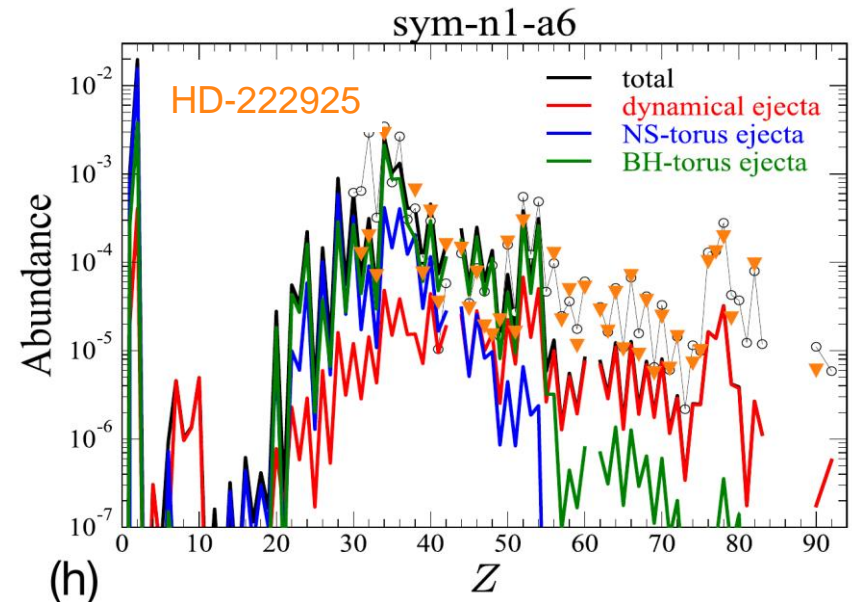
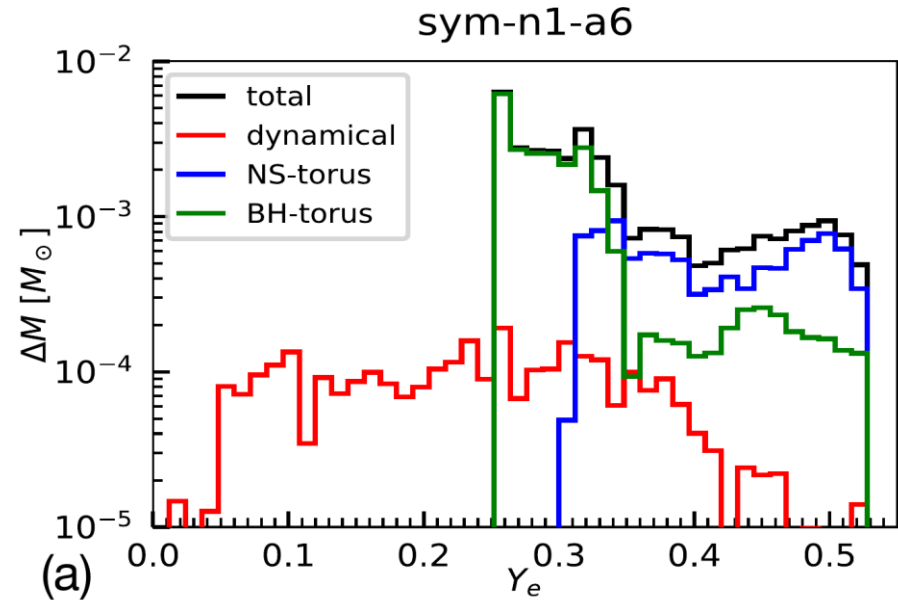
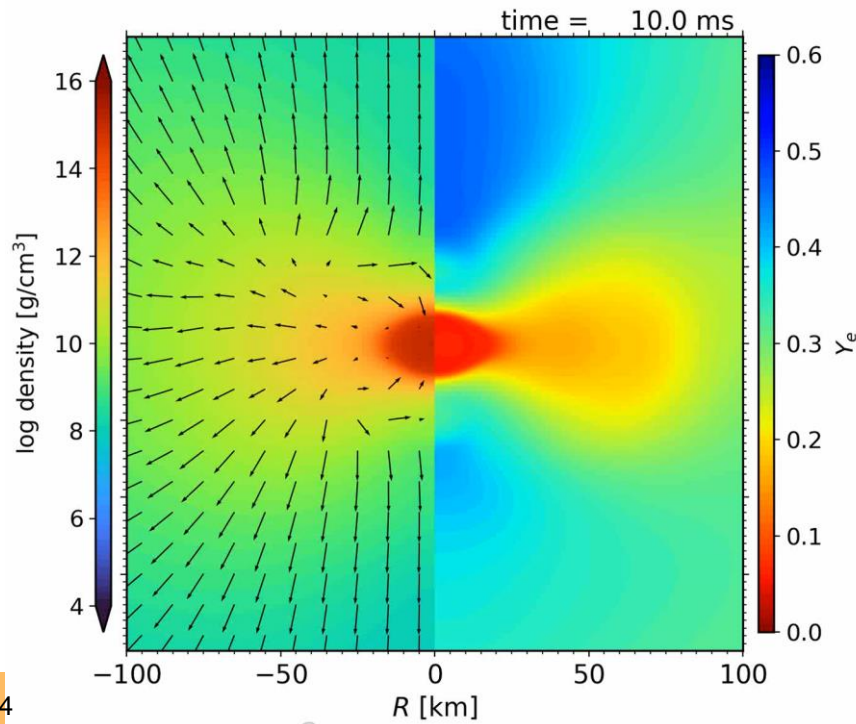


Long term merger simulations

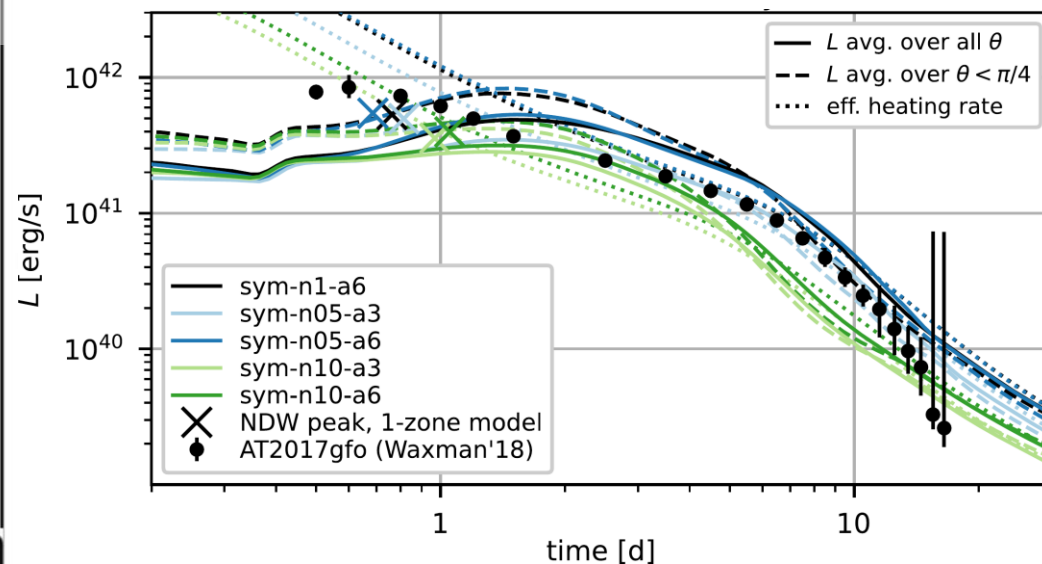
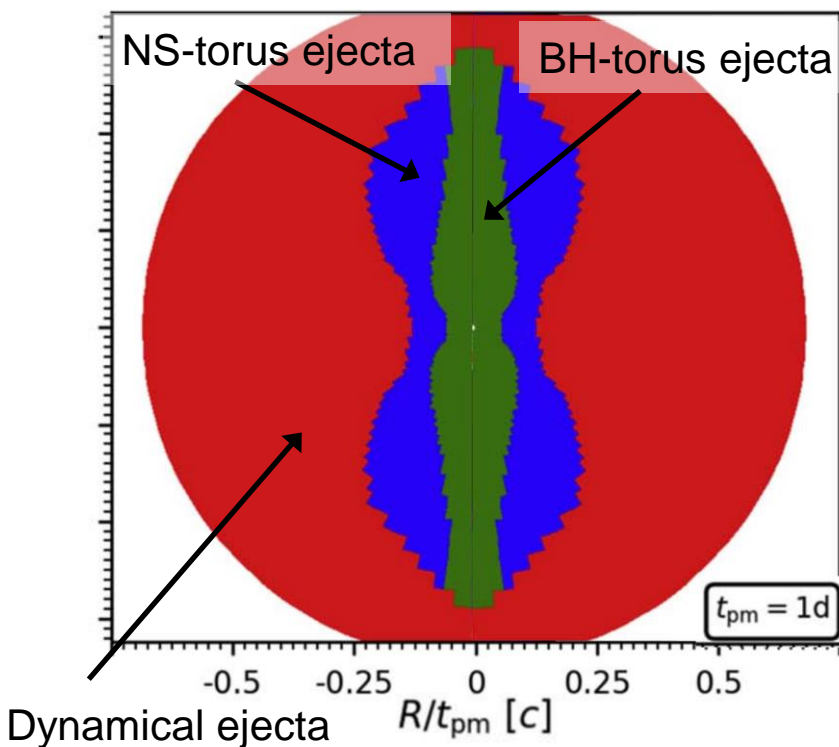
Long-term simulations with neutron star lifetimes 0.1-1 s and describe all components of the ejecta: dynamical, NS-torus ejecta, and final viscous ejecta from BH torus.



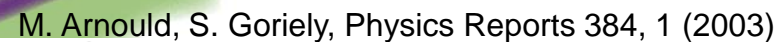
Just et al, ApJL, L12 (2023)



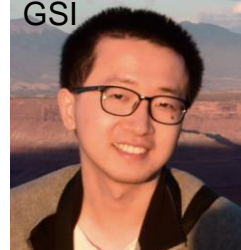
- Based on grey opacities using approximate radiative transfer model (generalization ALCAR neutrino module)
- Promising agreement with AT2017gfo after times of several days
- Accounting for all ejecta components fundamental to reproduce light curve



Just et al, ApJL, L12 (2023)



- Zewei Xiong
GSI



Possible source of light p-nuclei and ^{92}Nb

γ -process fails to produce light p-nuclei $^{92,94}\text{Mo}$ and $^{96,98}\text{Ru}$ in solar proportions (Raucher+2013)

Supernova neutrino winds:

- Ejecta with $Y_e \sim 0.48$ produce ^{92}Mo (Hofmann+1992)
- νp -process ($Y_e \gtrsim 0.55$) produces ^{94}Mo , $^{96,98}\text{Ru}$ (Fröhlich+2006)

Long-lived ^{92}Nb present in early solar system (Harper+1996).

Cannot be produced by the νp -process nor ν -process (Hayakawa+2013, Sieverding+2018)

Can we produce all these nuclei in the same environment including heavier p-nuclei?

	Rh 95	Rh 96	Rh 97	Rh 98	Rh 99	Rh 100	Rh 101	Rh 102	Rh 103	Rh 104	Rh 105
4 5.8 s	1.96 m 5.0 m	1.5 m 9.9 m	44 m 31 m	3.5 m 8.7 m	4.7 h 16 d	4.7 m 20.8 h	4.4 d 3.3 a	2.9 s 207 d	56.1 m 100	4.4 m 42 s	45 s 35.4 h
401: 3 3	γ 843 1952 784...	γ 33... 103... 1099 680 632 1699	γ 26... 103... 422 640 679	γ 652 103... 745... 652...	γ 87 103... 816 538 1261 353.90	γ 32: 74 103... 1540 2376 887... 1563	γ 387 103... 127 106 157 325	γ 475 103... 607 476 143 638	γ 40 103... 11 154	γ 51... 103... 1556 800	γ 6... 103... 1319 306 11000
3 8.7 s	Ru 94 51.8 m	Ru 96 1.65 h	Ru 97 5.54	Ru 97 2.9 d	Ru 98 1.87	Ru 99 12.76	Ru 100 12.60	Ru 101 17.06	Ru 102 31.55	Ru 103 39.35 d	Ru 104 18.62
53: 85:	γ 967; 891... m	ϵ : β^+ 1.2... γ 336; 1097; 627... g	α 0.23	γ 216; 324... g	α < 8	α 4	α 5.8	α 5	α 1.2	β^+ 0.2; 0.7... γ 497; 610... m	α 0.49
2 1	Tc 93 43.5 m	Tc 94 53 m	Tc 95 60 d	Tc 96 82 m	Tc 97 92.2 d	Tc 98 4.2 · 10 ⁹ a	Tc 99 6.0 h	Tc 100 15.8 s	Tc 101 14.2 m	Tc 102 4.9 m	Tc 103 54.2 s
3:	γ 362 1363 2545... 1477...	γ 0.8 1071 25... 871...	γ 0.8 1071 805 703 1074	γ 34 1071 778 850 1000... 913	γ 776 1071 897 no γ	β^- 0.4 γ 745; 652 α 0.9 + 7	γ 141... 1071 β^- 0.3 γ (90) γ (322)...	β^- 3.4... γ 540; 591...	β^- 1.3... γ 307; 545...	β^- 1.6; 3.2; γ 476 628... γ 476	β^- 2.2... γ 346; 136; 210...
1 1.5 m	Mo 92 14.77	Mo 93 6.9 h	Mo 94 9.23	Mo 95 15.90	Mo 96 16.68	Mo 97 9.56	Mo 98 24.19	Mo 99 66.0 h	Mo 100 9.67	Mo 101 14.6 m	Mo 102 11.2 m
337... 3	α 2E-7 + 0.06	γ 1477; 10 ⁹ a	α 0.02	α 13.4 α 0.000030	α 0.5	α 0.5 α 0.4E-7	α 0.14	β^- 1.2... γ 740; 182; 778... m; g	β^- 1.15 · 10 ¹⁰ a	β^- 0.8; 2.6... γ 192; 501; 1013; 506... g	β^- 1.1 γ 212; 148; 224... g
0 4.6 h	Nb 91 60.9 d	Nb 92 10.15 d	Nb 93 16.13 a	Nb 94 6.26 m	Nb 95 86.6 h	Nb 96 23.4 h	Nb 97 53 s	Nb 98 51 m	Nb 99 2.6 m	Nb 100 3.1 s	Nb 101 7.1 s
120: 9	γ 1105 1205	γ 581; 934	γ 311 1071	γ 0.8 1071	γ 0.8 1071	β^- 0.7... γ 776; 589; 1091	β^- 1.3... 1071	β^- 2.0; 2.9 γ 787; 1169	β^- 3.2... 1071 2642; 2854... 1365	β^- 3.1 γ 536; 600; 1200	β^- 4.3... γ 538; 538; 1200
9 14 h	Zr 90 51.45	Zr 91 11.22	Zr 92 17.15	Zr 93 1.5 · 10 ⁴ a	Zr 94 17.38	Zr 95 64.0 d	Zr 96 2.80	Zr 97 16.8 h	Zr 98 30.7 s	Zr 99 2.1 s	Zr 100 7.1 s
713: 3	α = 0.014	α 1.2	α 0.2	β^- 0.06... m	α 0.049	β^- 0.4; 1.1... γ 757; 724... m	β^- 1.9... γ 508; 1148; 355... m	β^- 1.9... γ 508; 1148; 355... m	β^- 2.3 no γ	β^- 3.5; 3.6... γ 469; 540; 594... g; m	β^- 2.6; 3.0 γ 504; 401... g
d	Y 89 16.9 s	Y 90 3.19 h	Y 91 49.7 m	Y 92 3.54 h	Y 93 10.1 h	Y 94 18.7 m	Y 95 10.3 m	Y 96 9.6 s	Y 97 1.2 s	Y 98 2.0 s	Y 99 0.55 s
100: 3	α = 0.001 + 1.25	β^- 2.3... γ (219)	β^- 1.3... γ (1205)	β^- 3.6... γ 934; 1405; 561; 449...	β^- 2.9... γ 267; 947; 1918...	β^- 4.9... γ 919; 1139; 551...	β^- 4.4... γ 954; 2178; 3577; 1324; 2633...	β^- 2.8... γ 1571; 1919 1107	β^- 4.8... γ 1000; 1000; 1000	β^- 4.8... γ 1000; 1000; 1000	β^- 4.8... γ 1000; 1000; 1000
50	50	52	54	56	58	60					

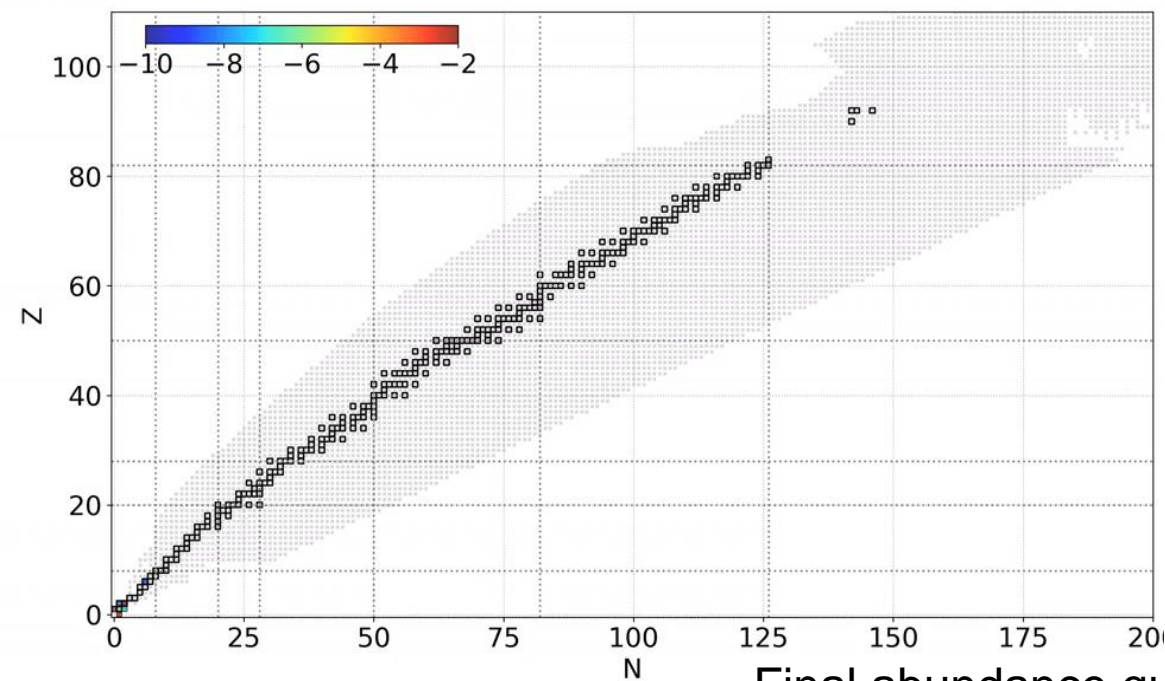
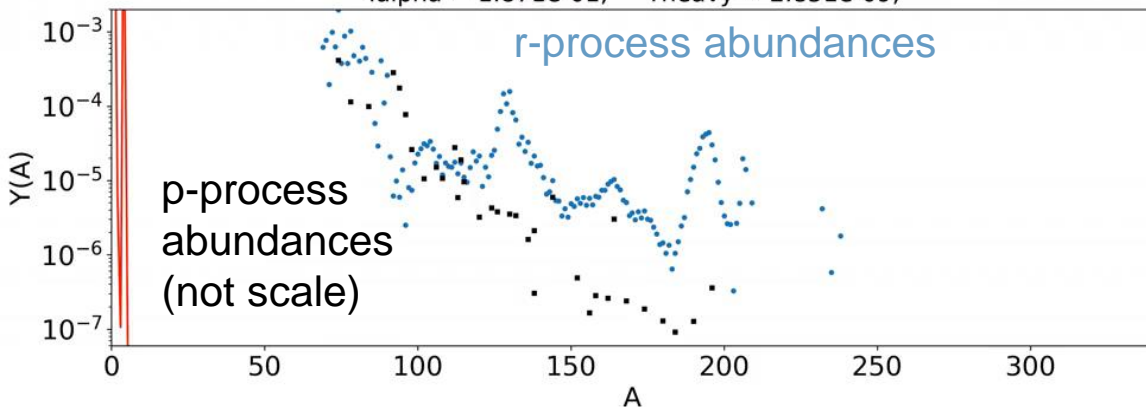
50 52 54 56 58 60

Phases during the operation of the vr-process

- **Seed production:** Strong neutrino fluxes drive material to $Y_e \sim 0.5$
- **Neutron-capture phase:** neutrons are used relatively fast by two competing mechanisms:
 - $n(\nu_e, e^-)p$ converts neutrons into protons that are captures in medium mass nuclei
 - $A(\nu_e, e^-X)$ $X = n, p, \alpha$ speeds up the decay of nuclei and the build up of heavy nuclei
- **Fast “decay” to stability and beyond:**
 $A(\nu_e, e^-X)$ reactions drive material to beta-stability and beyond
 - Neutrons, protons and alphas produced by both charged-current and neutral current spallation reactions.
 - Protons and alphas captured mainly in light nuclei
 - Equilibrium between $A(\nu_e, e^-X)$ and $A(n, \gamma)$ determines final abundance

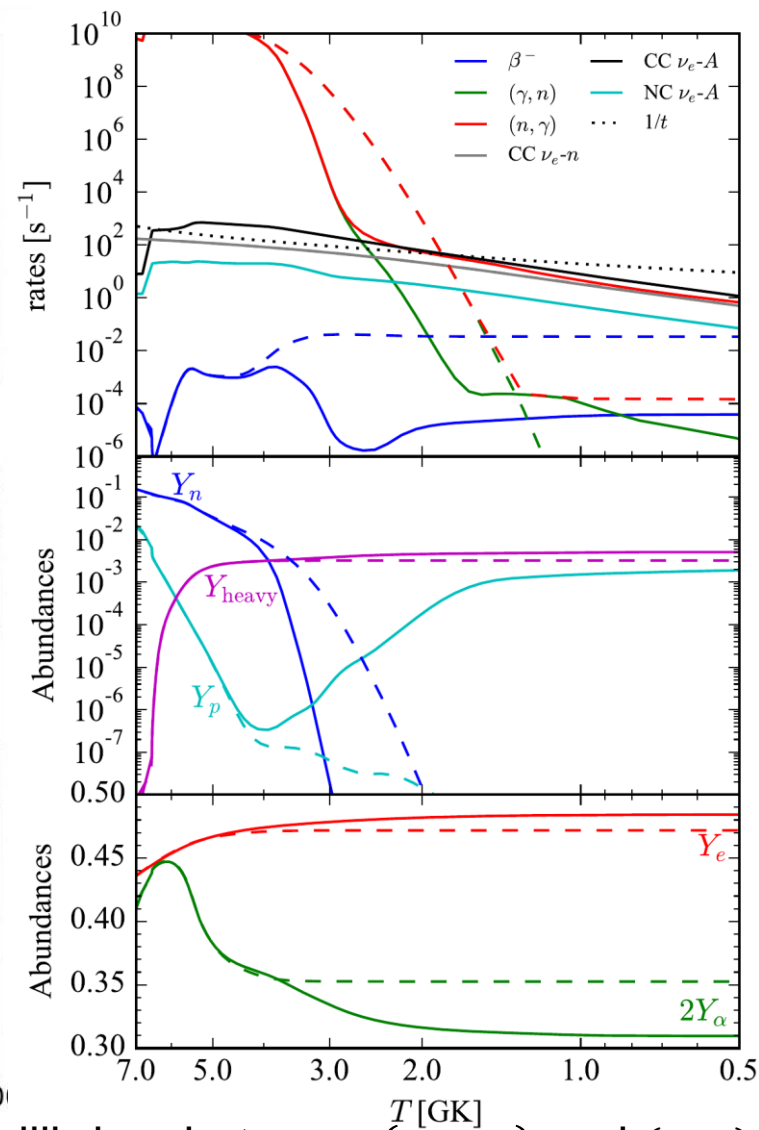
Nucleosynthesis (with neutrino-nucleus)

$i: 232; \quad t = 1.494\text{e-}03 \text{ s}; \quad T = 7.532\text{e+}00 \text{ GK}; \quad \rho = 1.791\text{e+}06 \text{ g cm-}^3;$
 $n_n = 2.152\text{e+}29 \text{ cm-}^3; \quad R_{n/s} = 7.002\text{e+}07; \quad S = 8.355\text{e+}01 \text{ kb/nuc};$
 $Y_e = 4.262\text{e-}01; \quad Y_n = 1.996\text{e-}01; \quad Y_p = 5.211\text{e-}02;$
 $Y_{\alpha} = 1.871\text{e-}01; \quad Y_{\text{heavy}} = 2.851\text{e-}09;$

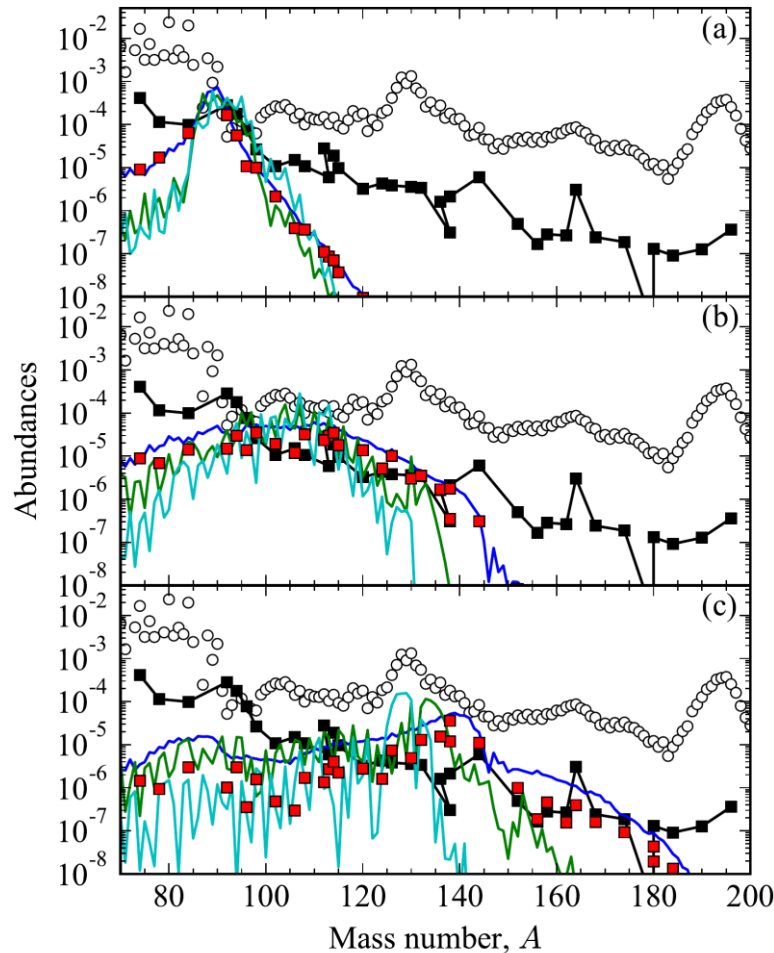


Final abundance equilibrium between (ν_e, e^-) and (n, γ)

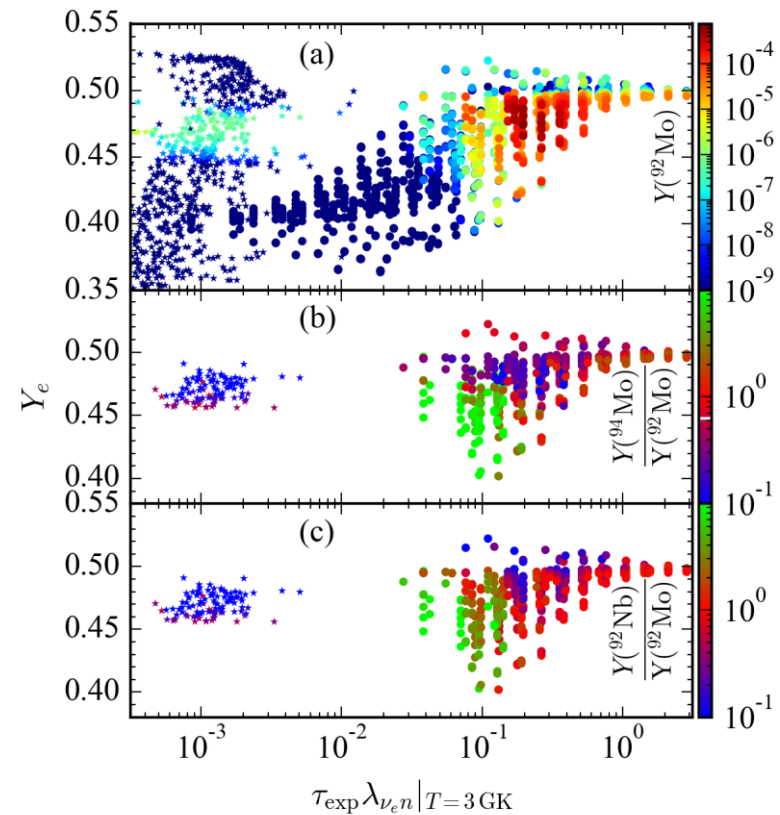
ν - A cross sections from
 Sieverding, et al, ApJ 865, 143 (2018).



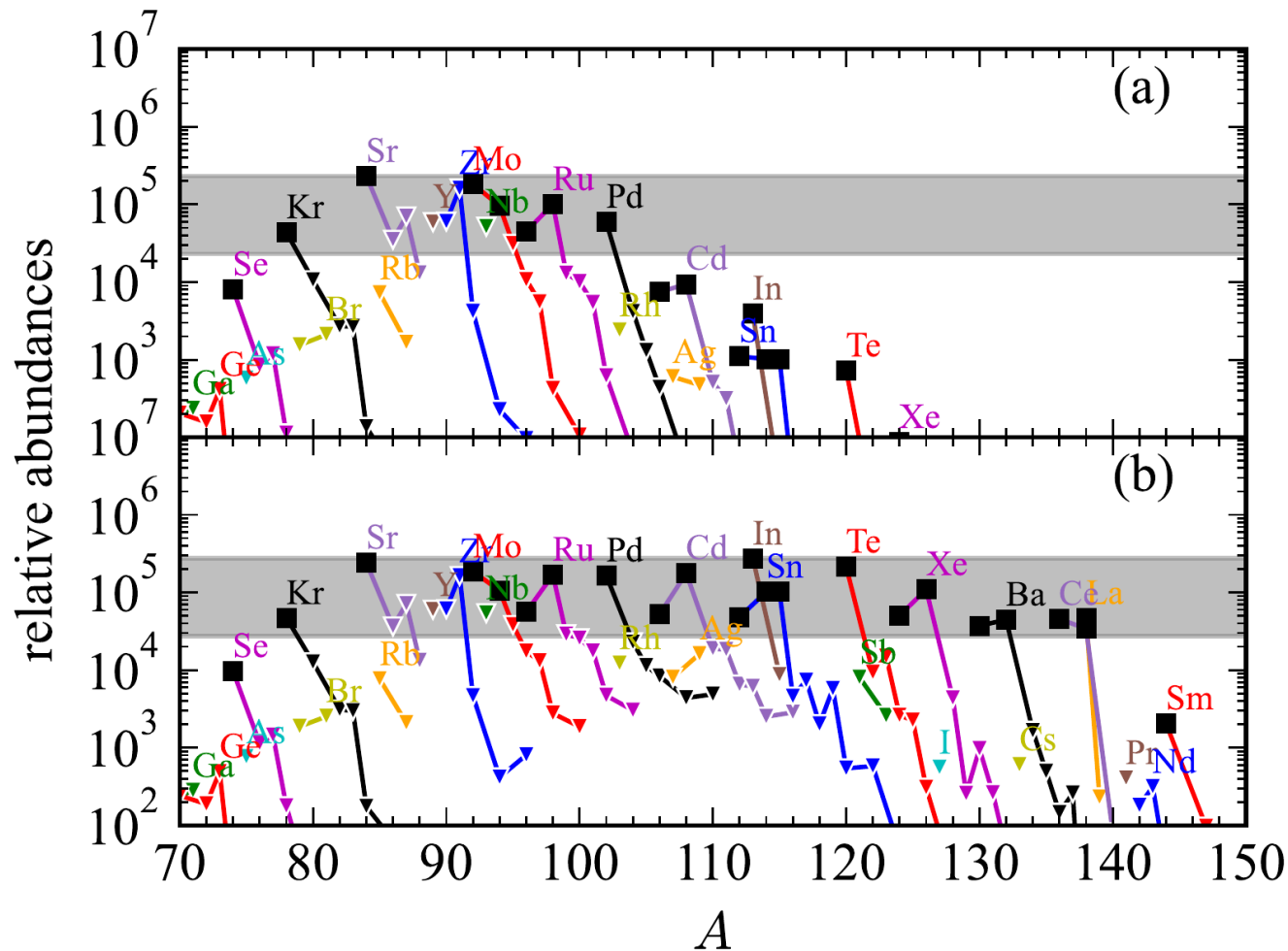
Increasing neutrino fluence allows to produce heavier p-nuclei



Dependence Y_e and neutrino fluence



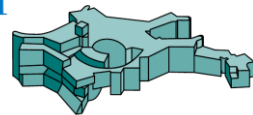
Current neutrino-hydrodynamical models are far from the necessary conditions
A non-thermal ejection mechanism is necessary (magnetic fields?)



- All p-nuclei can be consistently produced
- Assuming the same astrophysical site produces both r-process and p-nuclei around 1% of the ejecta should reach νr -process conditions

- Multi-messenger observations (Gravitational and Electromagnetic waves) from binary neutron star mergers provide unique opportunities to study the production of heavy elements:
 - Neutron star mergers identified as one astrophysical site where the r-process operates
 - Kilonova observations provide direct evidence of the “in situ operation of the r-process”
 - 3D radiative transfer allows to benchmark models with observations.
- Challenges:
 - Impact of weak processes and EoS in the ejecta properties
 - Improved nuclear and atomic input
 - Kilonova spectral modelling
- ν r-process: new mechanism production p-nuclei

Collaborators



Max-Planck-Institut für Astrophysik

A. Bauswein, **C. Collins**, A. Flörs,
O. Just, G. Leck, L. Shingles,
N. Rahman, **V. Vijayan**, Z. Xiong

P. Amaro, J. P. Marques, J. M. Sampaio,
R. Silva

S. Sim

J. Deprince, M. Godefroid, S. Goriely

H. Carvajal, P. Palmeri, P. Quinet

C. Robin

S. Giuliani, L. Robledo

A. Sieverding